Control of population transfer in degenerate systems by nonresonant Stark shifts

François Légaré*
Laboratoire de Chimie Théorique, Université de Sherbrooke, PQ, Canada, J1K 2R1
and National Research Council of Canada, Ottawa, Ontario, Canada K1A 0R6
(Received 3 August 2003; published 10 December 2003)

Two simple schemes are presented for the selective population transfer in systems where the target state is degenerate with a second level. Both states are coupled with the ground state via a one photon resonance. The schemes use a combination of two laser pulses. The first pulse breaks the degeneracy of the levels by inducing a Stark shift. The second pulse is chirped across the new levels. The idea is illustrated by numerical simulations of the time-dependent Schrödinger equation for a four-level system. The efficient population transfer is explained using a dressed state representation. In conclusion, applications for molecules are suggested.

DOI: 10.1103/PhysRevA.68.063403 PACS number(s): 32.80.Qk, 33.80.Gj, 07.05.Tp

I. INTRODUCTION

By controlling the time-dependent electric field of a laser pulse (amplitude and phase), one can control various processes in molecules [1,2]. One of the routes relies on controlling population transfer using an appropriate interference between quantum pathways. The efficiency of the control is determined by the ability to make this population transfer effective and selective. The simplest example for population inversion is the two-level system. By amplitude control, called a π pulse, a complete population inversion is achievable [3]. Another scheme relies on chirp (the time derivative of the phase), where a complete population transfer can be achieved by adiabatic passage, sweeping the frequency slowly across a resonance. This technique has been used for vibrational excitation of heteronuclear molecules [4,5] and electronic excitation [6]. Recently, Rickes *et al.* have proposed replacing phase modulation by an ac Stark shift [7].

For homonuclear molecules, where one-photon absorption within the same electronic state is forbidden by symmetry, the Raman effect has been used for population transfer between rovibrational states. The three level Λ system is the basic model for such a laser control scheme. Two different approaches have been proposed for population inversion in Λ systems, STIRAP [8] (stimulated Raman adiabatic passage) and CARP [9,10] (chirped adiabatic Raman passage). The first is resonant whereas the second can be resonant or nonresonant. STIRAP is based on a counterintuitive sequence of two laser pulses (with the pump pulse preceding the Stokes pulse), whereas CARP is achieved by slowly sweeping the frequency difference of a combination of two laser pulses across the anharmonicity of a rovibrational ladder. Recently, this idea has been used (and predicted) for the dissociation of diatomics by climbing the J, M_J ladder [11] and aligning excited vibrational states [12,13].

The current understanding of all these techniques of population inversion using coherent laser source applies to systems with nondegenerate quantum states, and with spacing between the final states large compared to the Rabi frequencies. In this paper, we consider the case of a degenerate V system and the possibility of controlling into which of the two degenerate upper states the population will be transferred. Recently, Shah *et al.* have shown that controllability in such a system is not possible [14] if there is no additional level. If the system has at least four levels and

$$\frac{\mu_{12}}{\mu_{24}} \neq \frac{\mu_{13}}{\mu_{34}}, \tag{1}$$

then the control is possible. μ_{ij} are the transition dipole moments between states i and j. This system is represented in Fig. 1. In this paper, two simple schemes based on chirp and induced Stark shifts are presented. Full population inversion from level 1 to level 2 (or 3) will be demonstrated by numerical simulation of the four-level time-dependent Schrödinger equation and the efficiency of the process is explained using the dressed state representation [15,16]. The key idea is that the fourth level can break the degeneracy of the levels. Strong nonresonant fields allow the energy shift to be large.

II. DESCRIPTION OF THE SYSTEM AND DRESSED STATE REPRESENTATION

The time-dependent Schrödinger equation for the system illustrated in Fig. 1 is written as follows:

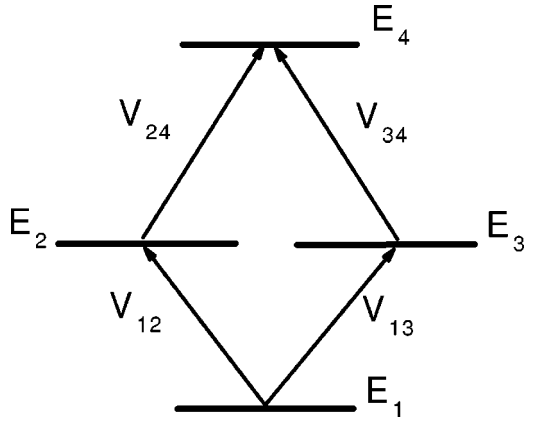

FIG. 1. Four-level system associated with Eq. (2). $V_{ij} = \mu_{ij}\mathcal{E}(t)$ and $\mu_{23}=0$.

*FAX: (613)-993-3437. Email address: francois.legare@nrc.ca

$$i\hbar\frac{\partial}{\partial t}\begin{bmatrix} a_1(t) \\ a_2(t) \\ a_3(t) \\ a_4(t) \end{bmatrix} = \begin{bmatrix} E_1 & V_{12}(t) & V_{13}(t) & 0 \\ V_{12}(t) & E_2 & 0 & V_{24}(t) \\ V_{13}(t) & 0 & E_3 & V_{34}(t) \\ 0 & V_{24}(t) & V_{34}(t) & E_4 \end{bmatrix} \times \begin{bmatrix} a_1(t) \\ a_2(t) \\ a_3(t) \\ a_4(t) \end{bmatrix}, \tag{2}$$

with $V_{ij}=\mu_{ij}\mathcal{E}(t)$. μ_{ij} are the dipole matrix elements. The time-dependent coefficients $a_i(t)$ are calculated using the Split Operator technique [17]. The time steps used in the integration of Eq. (2) are 1 a.u., which correspond to 0.0242 fs. Level 4 may represent a manifold of states with energies close to each other in comparison with the spacing between levels 2 and 3 and the manifold. In our model, $E_1=0$, $E_2=E_3=0.25$ a.u., and $E_4=0.55$ a.u. (1 a.u.$=27.21$ eV).

The electric field used for population inversion to level 2 (or 3) is the combination of an intense nonresonant laser pulse which Stark shifts the energy of the levels and a resonant laser pulse with the frequency chirped across the new Stark-shifted energies. The electric field is written as follows:

$$\mathcal{E}(t)=\mathcal{E}_{\rm nr}(t)\cos(\omega_{\rm nr}t)+\mathcal{E}_r(t)\cos\left(\omega_r t+\frac{1}{2}\beta t^2\right); \tag{3}$$

nr stands for the nonresonant laser pulse and r for the resonant laser pulse. $\mathcal{E}_{{\rm nr},r}(t)$ are the electric field envelope. The frequency of the nonresonant laser pulse, $\omega_{\rm nr}$, corresponds to wavelength of 800 nm (titanium sapphire). β is the chirp rate of the resonant pulse.

Before presenting results on exact numerical simulations, let us describe the physics of the proposed control schemes. First, the effect of the nonresonant laser pulse on the system can be included using perturbation theory. For levels 1 and 4, the energies are

$$e_1=E_1-\frac{\mathcal{E}_{\rm nr}^2}{4}\sum_{\pm}\left(\frac{\mu_{13}^2}{E_3-E_1\pm\hbar\omega_{\rm nr}}+\frac{\mu_{12}^2}{E_2-E_1\pm\hbar\omega_{\rm nr}}\right), \tag{4}$$

$$e_4=E_4-\frac{\mathcal{E}_{\rm nr}^2}{4}\sum_{\pm}\left(\frac{\mu_{24}^2}{E_4-E_2\pm\hbar\omega_{\rm nr}}+\frac{\mu_{34}^2}{E_4-E_3\pm\hbar\omega_{\rm nr}}\right). \tag{5}$$

For levels 2 and 3, the nonresonant coupling to levels 1 and 4 yields the following energies:

$$e_i=E_i-\frac{\mathcal{E}_{\rm nr}^2}{4}\alpha_{ii}, \tag{6}$$

with

$$\alpha_{ii}=\sum_{\pm}\left(\frac{-\mu_{i1}^2}{E_i-E_1\pm\hbar\omega_{\rm nr}}+\frac{\mu_{i4}^2}{E_4-E_i\pm\hbar\omega_{\rm nr}}\right). \tag{7}$$

Second, resonant Raman coupling between shifted levels has to be included exactly. The matrix element for such coupling is, since $E_2=E_3=E_{\rm int}$,

$$V_{23}=-\frac{\mathcal{E}_{\rm nr}^2}{4}\sum_{\pm}\left(\frac{\mu_{24}\mu_{34}}{E_4-E_{\rm int}\pm\hbar\omega_{\rm nr}}-\frac{\mu_{12}\mu_{13}}{E_{\rm int}-E_1\pm\hbar\omega_{\rm nr}}\right) =-\frac{\mathcal{E}_{\rm nr}^2}{4}\alpha_{23}. \tag{8}$$

Thus, the matrix in Eq. (2) can be reduced to a 3×3 matrix for levels 1–3, with nonresonant level 4 adiabatically eliminated:

$$i\hbar\frac{\partial}{\partial t}\begin{bmatrix} a_1(t) \\ a_2(t) \\ a_3(t) \end{bmatrix} = \left(\begin{bmatrix} E_1 & V_{12}(t) & V_{13}(t) \\ V_{12}(t) & E_2 & 0 \\ V_{13}(t) & 0 & E_3 \end{bmatrix} - \frac{\mathcal{E}_{\rm nr}(t)^2}{4}\begin{bmatrix} \alpha_{11} & 0 & 0 \\ 0 & \alpha_{22} & \alpha_{23} \\ 0 & \alpha_{23} & \alpha_{33} \end{bmatrix}\right)\begin{bmatrix} a_1(t) \\ a_2(t) \\ a_3(t) \end{bmatrix} = \begin{bmatrix} e_1 & V_{12}(t) & V_{13}(t) \\ V_{12}(t) & e_2 & V_{23}(t) \\ V_{13}(t) & V_{23}(t) & e_3 \end{bmatrix}\begin{bmatrix} a_1(t) \\ a_2(t) \\ a_3(t) \end{bmatrix}. \tag{9}$$

In Eq. (9), the resonant couplings are in the first matrix, and the nonresonant Stark shifts and Raman coupling are in the second matrix. The Raman coupling $V_{23}(t)$ gives two new Stark-shifted states. These energies are

$$e_\pm=\frac{e_2+e_3}{2}\pm\sqrt{(e_2-e_3)^2+4V_{23}^2}. \tag{10}$$

The eigenvectors associated with e_+ and e_- are

$$|e_+\rangle=\cos(\theta/2)|e_2\rangle+\sin(\theta/2)|e_3\rangle, \tag{11}$$

$$|e_-\rangle=-\sin(\theta/2)|e_2\rangle+\cos(\theta/2)|e_3\rangle, \tag{12}$$

with

$$\tan\theta=2\frac{\alpha_{23}}{\alpha_{22}-\alpha_{33}}. \tag{13}$$

The field free eigenvectors $|E_i\rangle$ are close to the Stark-shifted states $|e_i\rangle$ because of the nature of the nonresonant coupling. Note that $\tan\theta$ is *independent of the nonresonant field and is not changed after the field is turned off*. In order to understand our control scheme, we use the dressed state representation. The dressed state matrix in the rotating wave approximation is

$$\begin{bmatrix} \Delta_1(t) & \frac{1}{2}\Omega_{1-}(t) & \frac{1}{2}\Omega_{1+}(t) \\ \frac{1}{2}\Omega_{1-}(t) & e_- & 0 \\ \frac{1}{2}\Omega_{1+}(t) & 0 & e_+ \end{bmatrix}, \tag{14}$$

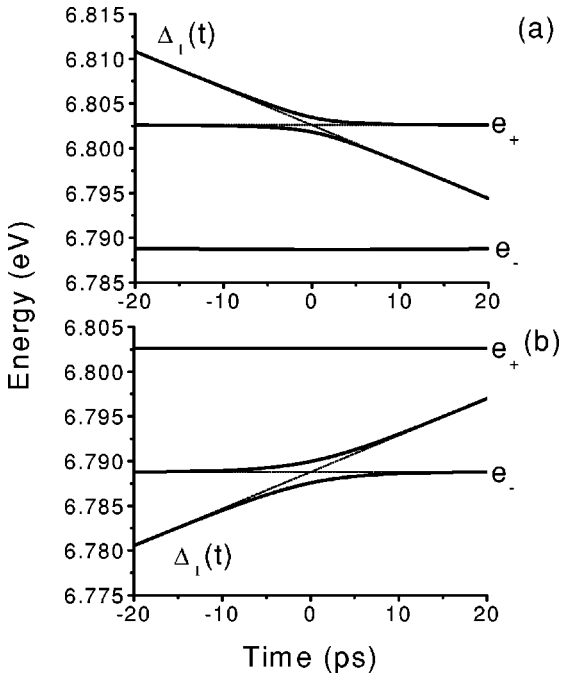

FIG. 2. Dressed state representation of scheme 1. (a) Population inversion to $|e_+\rangle(\approx|E_2\rangle)$. (b) Population inversion to $|e_-\rangle$ $(\approx|E_3\rangle)$.

with $\Omega_{1\pm}=\mu_{1\pm}\mathcal{E}_r(t)$, $\Delta_1(t)=e_1+\hbar\omega_r(t)$ and $\omega_r(t)=\omega_r+\beta t$. $\mu_{1\pm}$ are calculated using Eqs. (10)–(12). The diagonalization of the matrix gives the time dependent dressed states. Two schemes for efficient population transfer to these levels will be presented.

A. Scheme 1

The first scheme applies when $|\alpha_{33}-\alpha_{22}|\gg|\alpha_{23}|$. When such condition applies, the angle θ is close to zero and the Stark-shifted eigenvectors $|e_+\rangle$ and $|e_-\rangle$ are close to the field free states $|E_2\rangle$ and $|E_3\rangle$. Since θ is independent of the nonresonant field intensity, it is better to use a higher nonresonant field in order to increase the energy splitting between $|e_+\rangle$ and $|e_-\rangle$, and thus make it easier for the resonant field to distinguish the two Stark-shifted states energetically. A larger splitting also allows one to increase the chirp rate (and the resonant field) whole maintaining the adiabatic passage. Turning off the nonresonant field afterwards does not change the population transferred into the field-free degenerate states.

The dressed state representation associated with this scheme is presented in Figs. 2(a) and 2(b). In Fig. 2(a), the inversion of the population is from level 1 to level $|e_+\rangle$ $(\approx|E_2\rangle)$ and in Fig. 2(b) from level 1 to level $|e_-\rangle$ $(\approx|E_3\rangle)$. The nonresonant laser pulse for this control scheme has a plateau envelope and the resonant pulse has a Gaussian envelope of 20 ps [full width at half maximum (FWHM)] in the intensity profile. If the angle θ is far from zero, then this control scheme cannot be used. For example, if $|\alpha_{33}-\alpha_{22}|\ll|\alpha_{23}|$, then $|\theta|\approx\pi/2$ and the new states $|e_+\rangle$ and $|e_-\rangle$ are an equal superposition of the original states 2 and 3. Then, in order to achieve control, a different scheme can be used.

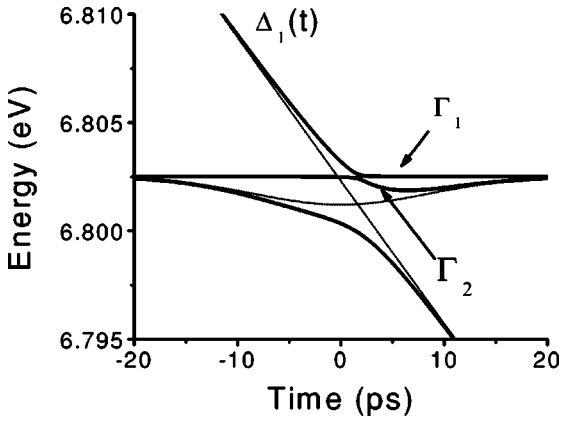

FIG. 3. Dressed state representation of scheme 2. By launching $\cos^2(\theta/2)$ of the population into the pathway Γ_1 and the rest into Γ_2, one can use the phase difference [Eq. (14)] to make on efficient population inversion to level 2 or 3.

B. Scheme 2

The second scheme is completely general when condition of Eq. (1) applies. The example that will be demonstrated in this paper is for $|\alpha_{33}-\alpha_{22}|\ll|\alpha_{23}|$. Nevertheless, the general condition for complete population transfer to any target state will be given. Note that in the limit $|\alpha_{33}-\alpha_{22}|\ll|\alpha_{23}|$, $|e_+\rangle$ and $|e_-\rangle$ are almost equal superpositions of $|E_2\rangle$ and $|E_3\rangle$.

Compared with the first scheme, instead of sweeping only across $|e_+\rangle$ or $|e_-\rangle$, the frequency of the resonant field is swept across both states. The nonresonant pulse has now a Gaussian envelope of 20 ps (FWHM) in the intensity profile, the same as the resonant pulse. In Fig. 3, the dressed state representation for this scheme is shown. The population starts in the level $|E_1\rangle$, and the adiabatic evolution of the corresponding dressed state is shown as path Γ_1. However, if the chirp rate is not too slow, a nonadiabatic transition at the avoided crossing makes a part of the population follow the path Γ_2. The phase difference between these two pathways [16,18] controls the population transfer at the end of the pulse. The phase difference is given by the following equation:

$$\Delta\phi=\int_{t_1}^{\infty}|\Gamma_2-\Gamma_1|dt. \tag{15}$$

The time t_1 is the time where the avoided crossing occurs. The condition for complete control can be established by rewriting the field free eigenvectors as a linear combination of $|e_+\rangle$ and $|e_-\rangle$:

$$|E_2\rangle\approx\cos\frac{\theta}{2}|e_+\rangle-\sin\frac{\theta}{2}|e_-\rangle, \tag{16}$$

$$|E_3\rangle\approx\cos\frac{\theta}{2}|e_+\rangle+\sin\frac{\theta}{2}|e_-\rangle. \tag{17}$$

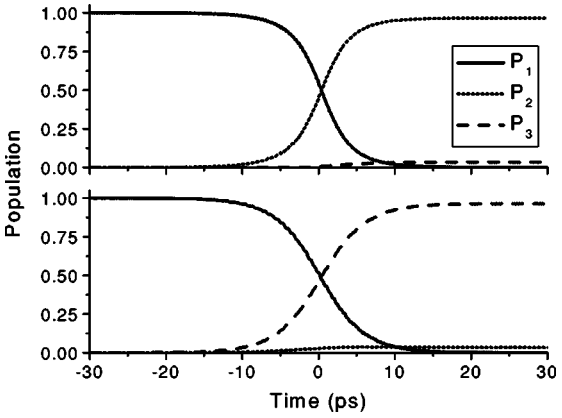

FIG. 4. Time-dependent population transfer for scheme 1. (a) See Fig. 2(a). (b) See Fig. 2(b).

To control the population, one can launch $\cos^2(\theta/2)$ into Γ_1 and $\sin^2(\theta/2)$ into Γ_2, which can be done by tuning the chirp rate (or the field) of the resonant laser pulse. Then, for the phase difference $\Delta\phi=\pi$ one would only populate $|E_2\rangle$, and for $\Delta\phi=2\pi$ all population will end up in $|E_3\rangle$. The phase difference $\Delta\phi$ is controlled by the intensity or the duration of the nonresonant laser pulse.

III. RESULTS AND DISCUSSION

A. Scheme 1

Without the presence of level 4, it has been demonstrated that the population ratio between levels 2 and 3 is given by $P_2/P_3=\mu_{12}^2/\mu_{13}^2$ [14,19]. Adding the fourth level (or a manifold of levels) allows one to control the population transfer. Consider first the case when the condition for scheme 1 are satisfied. The dipole matrix elements are $\mu_{12}=\mu_{13}=1$, $\mu_{24}=2$, and $\mu_{34}=10$. The dressed state representation is shown in Figs. 2(a) and 2(b). The intensity of the nonresonant pulse (plateau envelope) is 1×10^{11} W/cm^2, that of the resonant pulse is 2×10^8 W/cm^2 (Gaussian intensity profile with a 20-ps FWHM), and the chirp rate $|\beta|$ is 4.11×10^{-4} eV/ps. Because $\alpha_{33}-\alpha_{22}$ is much greater than the Raman matrix element $2\alpha_{23}$, $|e_-\rangle\approx|E_3\rangle$ and $|e_+\rangle\approx|E_2\rangle$. Then, by sweeping the resonant frequency across $|e_+\rangle$ or $|e_-\rangle$, efficient population transfer either to level 2 or 3 can be achieved.

In Fig. 4, results related to Fig. 2 are presented. A virtually full population inversion to any target state (2 or 3) is achieved in Fig. (4). The residual population in level 2 (or 3) for Fig. 4(a) [or (b)] is given by $P_{2(3)}=\sin^2(\theta/2)$ with θ given by Eq. (13). In our case, $\theta=-0.373$ rad and $P_{2(3)}=3.44\times10^{-2}$. The numerical simulation gives $P_3=3.51\times10^{-2}$ for Fig. 4(a) and $P_2=3.42\times10^{-2}$ for Fig. 4(b), close to our analytical prediction. Note that the Rabi frequency of the resonant pulse has to be small compared with $|e_+-e_-|$. With the condition enumerated in the previous paragraph, the ratio between $|e_+-e_-|$ and the Rabi frequency is approximately 10. Since θ is independent of the intensity of the non-resonant laser pulse, high intensity should be used so large Rabi frequency for the resonant laser pulse can also be used in order to sweep rapidly the frequency of the resonant laser pulse [16], making the process as fast as possible while still satisfying the adiabatic condition.

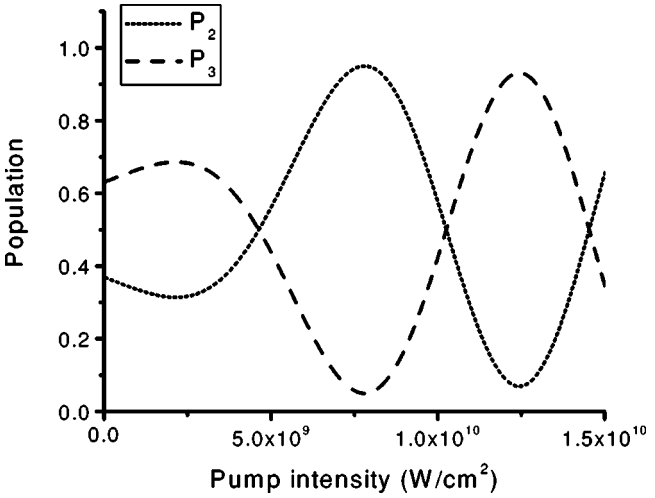

FIG. 5. Final population in level 2 and 3 for scheme 2. The x axis is the intensity of the nonresonant laser pulse.

B. Scheme 2

In the case of scheme 2, the dressed state representation is shown in Fig. 3. The dipole matrix elements are: $\mu_{24}=\mu_{34}=5$, $\mu_{12}=0.8$ and $\mu_{13}=1$ and the intensity of the nonresonant pulse (Gaussian intensity profile with a 20-ps FWHM) is a control parameter. Tuning the intensity of this pulse changes the phase difference [Eq. (14)] between the two pathways in Fig. 3 and tuning the chirp rate (or the field) of the resonant laser pulse makes the right superposition of the amplitudes launch into pathways Γ_1 and Γ_2. The intensity of the resonant laser pulse is 2×10^8 W/cm^2 (Gaussian intensity profile with a 20-ps FWHM) and the chirp rate β is -6.61×10^{-4} eV/ps. Because $\mu_{24}=\mu_{34}$, $|\alpha_{33}-\alpha_{22}|$ is small compared to the Raman coupling $2|\alpha_{23}|$, the angle θ [Eq. (12)] is approximately equal to $-\pi/2$. Then, the eigenvectors given by Eqs. (10) and (11) are: $|e_+\rangle\approx(|E_2\rangle-|E_3\rangle)/\sqrt{2}$ and $|e_-\rangle\approx(|E_2\rangle+|E_3\rangle)/\sqrt{2}$. If μ_{12} converges to μ_{13}, then $|e_+\rangle$ approaches more and more a dark state [20] and the control becomes difficult to achieve; see Eq. (1). In our case, the controllability condition is satisfied since $\mu_{12}\neq\mu_{13}$. In the *real world*, the nonequality condition will be always satisfied because two degenerate states have different quantum numbers, making for example the Clebsh-Gordan coefficients different. Then, by making an appropriate coherent superposition of $|e_-\rangle$ and $|e_+\rangle$, population can be transferred to either level 2 or level 3. In Fig. 5, the numerical results associated with the scheme of Fig. 3 are presented. They confirm the validity of the control scheme.

IV. CONCLUSION

From numerical solutions of the time-dependent Schrödinger equation for a four state system, it is shown that population inversion in the presence of degeneracy can be controlled using laser induced Stark shifts. Two schemes have

been presented. Both schemes use a combination of two laser pulses, one nonresonant (intense) and another resonant. The intense pulse breaks the degeneracy of the system and the second one is swept (chirped) across the new energies. A complete general formulation requires only a knowledge of the Stark matrix of couplings to the nonresonant laser field: α_{22}, α_{33}, and α_{23}. The two cases studied in this paper are $|\alpha_{23}| \ll |\alpha_{33} - \alpha_{22}|$ (scheme 1) and $|\alpha_{23}| \gg |\alpha_{33} - \alpha_{22}|$ (scheme 2). Scheme 1 is only efficient when condition (1) applies. Scheme 2 is completely general and the condition for complete inversion to any target state is defined using Eqs. (15)–(17).

The first scheme uses the difference between the coupling of the degenerate states to a manifold of states (the fourth level). Because of the different coupling, these degenerate states move differently in the presence of the intense laser field. By sweeping the resonant frequency across one of the new Stark-shifted states, an efficient population inversion can be achieved for any of the two target states.

The second scheme uses the phase difference between the two pathways created by the nonresonant laser pulse. By sweeping the frequency of the resonant photon across these two pathways and by launching $\cos^2(\theta/2)$ into Γ_1 and $\sin^2(\theta/2)$ into Γ_2, an efficient population inversion can be obtained by tuning the phase difference using the intensity of the nonresonant laser pulse as the control variable.

A coherent control of population inversion in degenerate system is of interest in photochemistry [21]. Often, fragmentation channels are degenerate [22] and using only resonant laser pulses yields population ratios associated with the dipole moment ratio [14,19]. In the present model, discrete states are used as compared to multiple or quasidegenerate continua in real systems. The first scheme, which uses only a Stark shift, should be easier to implement experimentally. Scheme 2 is strongly phase dependent, and one can expect that it would be more difficult to implement in practice, especially for systems with continua where couplings are energy dependent. On the other hand, scheme 2 will be efficient in atomic systems, where a similar interference scheme has been used to control the atomic population inversion [18]. An extension to molecular degenerate systems will require further numerical simulations for establishing the limitation of this control scheme which is based on differentiating the level via their Stark shifts, which is essential for controlling population transfer in system where the target states are degenerate.

ACKNOWLEDGMENTS

F.L. thanks NSERC and FQRNT for grants supporting the present research. Also, F.L. thanks Dr. A. D. Bandrauk at Université de Sherbrooke, B. Sussman, Dr. M. Yu. Ivanov, and Dr. P. B. Corkum at NRC Ottawa for stimulating discussions.

[1] M. Shapiro and P. Brumer, Rep. Prog. Phys. **66**, 859 (2003).
[2] A. D. Bandrauk, Y. Fujimura, and R. J. Gordon, *Laser Control and Manipulation of Molecules*, ACS Symposium No. 821 (American Chemical Society, Washington, D.C., 2003).
[3] J. Allen and J. H. Eberly, *Optical Resonance and Two-Level Atoms* (Wiley, New York, 1975).
[4] S. Chelkowski, A. D. Bandrauk, and P. B. Corkum, Phys. Rev. Lett. **65**, 2355 (1990).
[5] V. D. Kleiman, S. M. Arrivo, J. S. Mellinger, and E. J. Heilweil, Chem. Phys. **233**, 207 (1998).
[6] J. C. Cao, C. J. Bardeen, and K. R. Wilson, Phys. Rev. Lett. **80**, 1406 (1998).
[7] T. Rickes, L. P. Yatsenko, S. Steuerwald, T. Halfmann, B. W. Shore, and K. Bergmann, J. Chem. Phys. **113**, 534 (2000).
[8] K. Bergmann, H. Theuer, and B. W. Shore, Rev. Mod. Phys. **70**, 1003 (1998).
[9] S. Chelkowski and G. Gibson, Phys. Rev. A **52**, R3417 (1995).
[10] S. Chelkowski and A. D. Bandrauk, J. Raman Spectrosc. **28**, 459 (1997).
[11] D. M. Villeneuve, S. A. Aseyev, P. Dietrich, M. Spanner, M. Yu Ivanov, and P. B. Corkum, Phys. Rev. Lett. **85**, 542 (2000).
[12] F. Légaré, S. Chelkowski, and A. D. Bandrauk, Chem. Phys. Lett. **329**, 469 (2000).
[13] A. D. Bandrauk, S. Chelkowski, and F. Légaré, *Recent Research Developments in Raman Spectroscopy* (Transworld Research Network, Trivandrum, India, 2002), pp. 83–104.
[14] S. P. Shah, D. J. Tannor, and S. A. Rice, Phys. Rev. A **66**, 033405 (2002).
[15] A. D. Bandrauk, *Molecules in Laser Fields* (Dekker, New York, 1994).
[16] F. Légaré, S. Chelkowski, and A. D. Bandrauk, J. Raman Spectrosc. **31**, 15 (2000).
[17] A. D. Bandrauk and H. Shen, J. Chem. Phys. **99**, 1185 (1993).
[18] D. J. Maas, C. W. Rella, P. Antoine, E. S. Toma, and L. D. Noordam, Phys. Rev. A **59**, 1374 (1999).
[19] M. N. Kobrak and S. A. Rice, Phys. Rev. A **57**, 2885 (1998).
[20] P. Král and M. Shapiro, Phys. Rev. A **65**, 043413 (2002).
[21] Z. Chen, M. Shapiro, and P. Brumer, Phys. Rev. A **52**, 2225 (1995).
[22] S. S. Brown, R. B. Metz, H. Laine Berghout, and F. Flemiing Crim, J. Chem. Phys. **105**, 6293 (1996).